Elucidation of coordination structure around Ce^{3+} in doped SiO_2 glasses using pulsed electron paramagnetic resonance: Effect of phosphorus, boron, and phosphorus-boron codoping

Akira Saitoh,[1] Satoru Matsuishi,[1] Masanori Oto,[2,3] Taisuke Miura,[3] Masahiro Hirano,[3] and Hideo Hosono[1,3]
[1]*Frontier Collaborative Research Center, Tokyo Institute of Technology, Nagatsuta, Midori-ku, Yokohama 226-8503, Japan*
[2]*Showa Electric Wire and Cable, Minami-Hashimoto, Sagamihara 299-1133, Japan*
[3]*ERATO-SORST, Japan Science and Technology Agency, Frontier Collaborative Research Center, Tokyo Institute of Technology, Nagatsuta, Midori-ku, Yokohama 226-8503, Japan*
(Received 18 August 2005; revised manuscript received 26 October 2005; published 9 December 2005)

Effects of codoping of phosphorus and/or boron on the coordination sphere of a Ce^{3+} in SiO_2 glasses were examined by applying pulsed electron paramagnetic resonance (EPR) electron spin echo envelope modulation (ESEEM) spectroscopy. Simulation of the observed ESEEM pattern revealed a striking difference in the solvation shell structure between the P-doped and the P-free glasses, i.e., the P doping is very effective for the formation of the solvation shell, while no such an effect was observed for the B doping. When P and B are simultaneously doped, the solvation shell structure is close to that in the P-doped samples. Photoluminescence properties of Ce^{3+} in these samples were found to be classified into two categories corresponding to the solvation shell structures.

DOI: 10.1103/PhysRevB.72.212101 PACS number(s): 61.43.Bn, 61.43.Fs, 61.18.Fs, 78.55.Qr

Silica (SiO_2) glasses doped with rare earth (RE) ions are widely employed in applications for optical devices. However, constitution of the coordination structure around RE ions in doped SiO_2 glasses remains unclear. Although SiO_2 glass that has many excellent physical properties[1–4] is a highly desired host for optically active ions, its fatal drawback is poor solubility of multivalence cations such as RE ions, i.e., doped RE ions easily make a cluster in pure SiO_2 glass. It is suggested that the creation of a nonbridging oxygen facilitates pairing of the RE ions, leading to the formation of nanoclusters, which results in the concentration quenching of luminescence. This issue was resolved by a codoping technique.[5–7] Arai *et al.*[7] proposed the "solvation-shell" model based on the observation of luminescence properties of Nd^{3+} and Ce^{3+} ions in SiO_2 glasses for the understanding of striking codoping effects. The concept of solvation shell of ions in the glass, i.e., preferential coordination of dopant around a RE ion is very favorable for designing highly efficient optical material. However, little quantitative and concrete information on the solvation structure has been reported to date.[8] The purpose of this study is to clarify the effect of the codoping of phosphorus and boron on the formation of the solvation structure around a RE ion in SiO_2 glasses by determining the medium range structure around a RE^{3+} ion. A Ce^{3+} ion was chosen as a RE ion for this purpose because it is a sensitive indicator to monitor the solvation structures and a most promising active ion for ultraviolet (UV) fiber lasers.

Synthetic SiO_2 glasses codoped with Ce^{3+} ions and codopants, P_2O_5 and B_2O_3, were fabricated by a conventional modified chemical vapor deposition method. Ce^{3+} ions were doped by dipping the soot into a methanol solution of $CeCl_3$. Table I summarizes chemical compositions of the samples used in this study.

Photoluminescence (PL) and photoluminescence excitation (PLE) spectra of the codoped SiO_2 glasses were measured using a conventional fluorescence spectrophotometer at room temperature. PL lifetime was measured with a streak camera attached to a spectrometer using a fourth harmonic of a Nd:YAG (yttrium aluminum garnet) laser as an excitation light source. Pulsed-EPR experiments were performed using an *X*-band spectrometer (Bruker, E580) equipped with a dielectric resonator in an Oxford instrument cryostat for detection of unresolved hyperfine splitting due to the weak coupling between the unpaired electron spin and the nucleus spin.[9]

Calculation of an ESEEM spectrum was carried out by numerical diagonalization of the rotating spin Hamiltonian composed of a hyperfine, nuclear-Zeeman, and nuclear quadrupole interactions since the nuclear-quadrupolar coupling constant e^2qQ_n/h is comparable to the nuclear-Zeeman energy $g_n\beta_nH_0/h$ in a boron-nucleus case. Detailed simulation algorithms employed were described in the preceding paper.[10]

Figure 1 shows PL and PLE spectra of four types of the samples. The P^{5+}-ion-codoped glass samples (CPS and CPBS) exhibit PL bands peaking at ~350 nm and ~325 nm, while the P^{5+}-ion-free samples (CBS and CS) show PL bands at ~420 nm and ~435 nm, respectively. The PL decay time was classified into two groups, i.e., 25–36 ns for the P-doped samples (CPS and CPBS), and 58–74 ns for the P-free samples (CBS and CS).

Figure 2 shows the observed three-pulsed ESEEM spectrum of the Ce^{3+}-doped SiO_2 glass (CS) along with the calculated spectrum. Although the modulation amplitude was rather low (less than 0.3%), it is evident from the Fourier-

TABLE I. Samples. The dopant concentration was determined by an electron probe microanalyzer.

Sample	Composition (mol %)
CS	0.04 Ce_2O_3-100SiO_2
CBS	0.02 Ce_2O_3-3B_2O_3-97SiO_2
CPS	0.004 Ce_2O_3-1P_2O_5-99SiO_2
CPBS	0.004 Ce_2O_3-3P_2O_5-8B_2O_3-89SiO_2

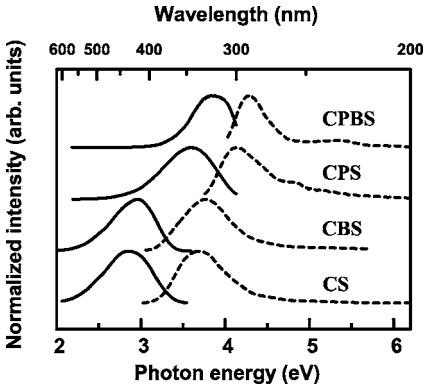

FIG. 1. Photoluminescence (PL: left) and photoluminescence excitation (PLE: right) of Ce^{3+}-activated SiO_2 glasses at room temperature.

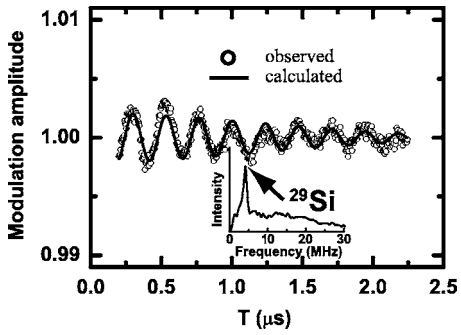

FIG. 2. Observed and simulated three-pulsed ESEEM spectra of a CS sample. Inset is the FT-ESEEM pattern of the observed spectrum. An arrow denotes the NMR frequency of the responsible magnetic nucleus. The measurement conditions; $\tau=172$ ns, $H_0=500$ mT, and temperature=4 K. The calculation was carried out for the case that 21 Si^{4+} ions ($20\times{}^{28}Si+1\times{}^{29}Si$) are positioned uniformly in the range 0.3–1.2 nm around a Ce^{3+}. The standard deviation between the observed and calculated spectra is 0.63%.

transformed spectrum (inset of Fig. 2) that the signal came from the ^{29}Si nucleus ($I=1/2$, natural abundance 4.7%). Here, we calculated the ESEEM pattern due to the ^{29}Si nucleus under the uniform distribution model. The effective range of r (separation) for ESEEM is taken as 0.3 to 1.2 nm because the shorter r should give a resolved hyperfine splitting and the longer r does not contribute to the observed oscillation pattern. The number (N_i) of ^{29}Si nucleus locating in the ith slice (thickness of each slice Δr is taken as 0.05 nm, i.e., r is divided into 18 slices) of the coordination sphere around Ce^{3+} is given by the following equation:

$$N_i = N_{avog} \times \frac{\rho}{M} \times C \times \frac{4\pi}{3}\{(r_j+\Delta r)^3-(r_j-\Delta r)^3\}, \quad (1)$$

where $i=1,2,\ldots$, and 18, N_{avog} Avogadro's number, ρ the density of sample, M atomic weight of ^{29}Si, and C the natural abundance of ^{29}Si. The ESEEM pattern is calculated by using each set of ($N_i r_i$).

Figure 3 shows the observed ESEEM spectrum of the Ce^{3+}-P^{5+}-codoped SiO_2 (CPS). The FT-ESEEM spectrum (inset) indicates the signal is due to ^{31}P ($I=1/2$, n.a.=100%) nucleus. The best fitted pattern calculated for the uniform distribution of P^{5+} ions ($C_P\sim 2$ mol %) around a Ce^{3+} was distinctly different from the observed spectrum. A better pattern was shown by the solid curve which was obtained by a model in which a Ce^{3+} is preferentially coordinated by four PO_4 units (the total number of P^{5+}; $N_P=4$). There are two types of P ions coordinating to a Ce^{3+} ion through oxygens in crystalline $CePO_4$,[11] i.e., an edge-sharing type and a corner-sharing type. The separation between the Ce^{3+} and the P^{5+} ion is $\sim$0.3 nm for the edge sharing or $\sim$0.4 nm for the corner sharing. We sought a best fit by the trial-and-error method, keeping in mind this structural information. As a result, a best fit between the observed and calculated spectra was found by assuming that there were two types of the separation between Ce^{3+} and P^{5+} ions: distance r_{P1} between Ce^{3+}-P_1^{5+} ions (numbers of P_1^{5+}; $N_{P1}=2$) and r_{P2} between Ce^{3+}-P_2^{5+} ions (numbers of P_2^{5+}; $N_{P2}=2$). Figure 3 shows a structural model around a Ce^{3+} in CPS. Here we assumed that each Ce^{3+} is coordinated by eight oxygens in

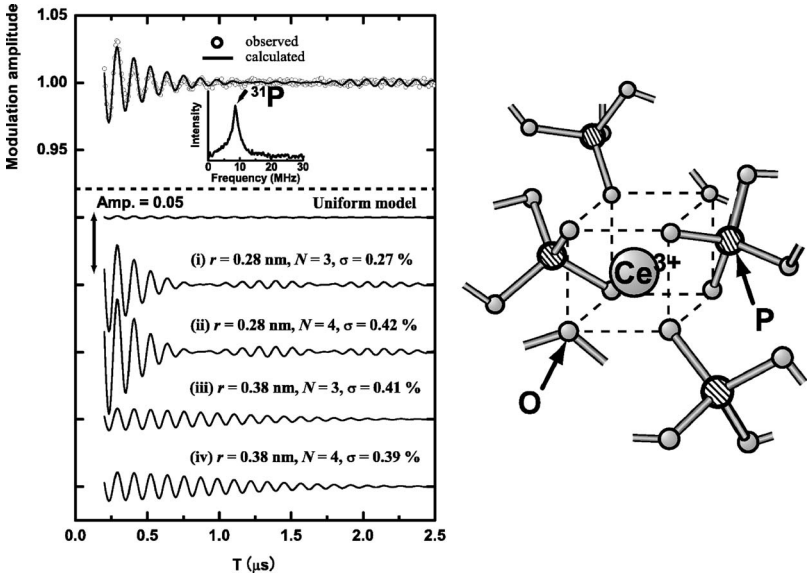

FIG. 3. Observed and calculated ESEEM patterns for CPS sample (left) and the coordination structure model deduced from the simulation (right). The measurement conditions; $\tau=172$ ns, $H_0=500$ mT, and 4 K. (Top) observed pattern, best-fitted pattern, and the pattern calculated for the uniform distribution of P ions. The best-fitted curve was obtained by assuming that two P ions are positioned at $r=0.28$ nm and two P ions are located at $r=0.38$ nm. (Bottom) ESEEM patterns calculated for various sets of Ce^{3+}-P^{5+} distance r and phosphorus number N (denoted in) The contribution from the range 0.6–1.2 nm around a Ce^{3+} was incorporated in each calculation using a uniform distribution of the magnetic nucleus (^{31}P). The standard deviation σ for each fitting is shown.

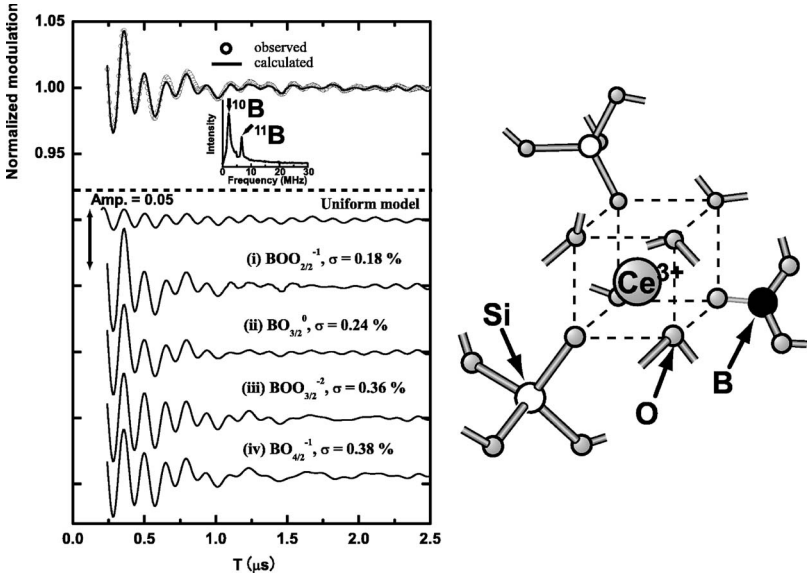

FIG. 4. Observed and calculated ESEEM patterns for a CBS sample (left) and the deduced structural model (right). The measurement conditions; τ=80 ns, H_0=500 mT, and 4 K. (Top) the observed pattern, the best-fitted pattern, and the pattern calculated for uniform distribution of boron. The best fit was obtained by assuming the case that B^{3+} ion of 0.8 is positioned at 0.30 nm, and the quadrupolar coupling constant e^2qQ_n/h of 4.97 MHz for a ^{10}B or 2.45 MHz for a ^{11}B nucleus, and the asymmetry parameter η is 0.59. The value σ for the fitting is 0.18%. (Bottom) patterns calculated for different borate ligands positioned at 0.30 nm.

all samples throughout this paper. The bottom part of the figure shows the four ESEEM patterns calculated by changing r and N of P^{5+} ions. However, neither of these patterns gave a better fit than the calculated curve in the top. It is thus concluded that the coordination model composed of two P^{5+} positioned at 0.28 nm and two P^{5+} at 0.38 nm gives the best fit with the observed ESEEM spectrum.

Figure 4 shows the observed ESEEM spectrum of the Ce^{3+}-B^{3+}-codoped SiO_2 (CBS) glass along with a calculated pattern. The inset shows the Fourier transform (FT) spectrum showing two peaks corresponding to ^{10}B (I=3, n.a.=19.8%) and ^{11}B (I=3/2, n.a.=80.2%). First, we calculated the ESEEM pattern for the uniform distribution of B^{3+} ions in the range 0.3–1.2 nm. The intensity of the calculated pattern is too small to be fitted to the observed pattern. The best fit was sought by a trial-and-error method in changing the r, N, e^2qQ_n/h and η, keeping possible boron units such as $BO\emptyset_{2/2}^{-1}$ and $B\emptyset_{4/2}^{-1}$ in mind. The former is a triangle borate unit with a nonbridging oxygen (O) and the latter is a tetrahedral borate unit with four bridging oxygens (Ø). According to NMR studies of B nucleus,[12–15] these two units can be distinctly distinguished in the value of the quadrupolar coupling constant (e^2qQ_n/h) and the asymmetric parameter (η). The value of e^2qQ_n/h was 4.8–5.8 MHz for ^{10}B, or 2.4–2.9 MHz for ^{11}B nuclei, and η was 0.59 for the triangle borate with a nonbridging oxygen.[12] On the other hand, the values of e^2qQ_n/h were 0–2.0 MHz for ^{10}B nucleus, and η was zero for the tetrahedral borate with four bridging oxygens.[12] The bottom part of the figure shows patterns calculated for four types of borate units. The coordination of the triangle borate with a nonbridging oxygen $BO\emptyset_{2/2}^{-1}$, case (i), gives the best fitted pattern, while the others, (ii)–(iv), rather deviate from the observed spectrum. Therefore, the model for CBS was determined as Fig. 4 (right); a triangle borate with a nonbridging oxygen ($BO\emptyset_{2/2}^{-1}$) positioned at 0.3 nm from a Ce^{3+} coordinates to the Ce^{3+}. The total numbers of B^{3+} ions within the sphere of a 0.6 nm radius under a uniform distribution model were estimated to be 0.8 by putting dopant concentration of B_2O_3 ($C_B \sim 3$ mol %) into Eq. (1). This value is close to the observation (N_B=0.8).

Figure 5 shows the observed ESEEM spectrum of the Ce^{3+}, (P^{5+}+B^{3+})-codoped SiO_2 (CPBS). The inset is of the FT spectrum showing three peaks corresponding to NMR frequencies of ^{31}P, ^{10}B, and ^{11}B nuclei. The early part in the time-domain was similar to that of CPS, indicating that the values of r for Ce^{3+}-P^{5+} and N of P^{5+} are close to those in CPS. On the other hand, the latter part was similar to that of CBS. In addition, it was suggested that some of the B^{3+} ions are positioned considerably far from a Ce^{3+} because a distinct modulation was observed in the long time region. Therefore, we first employed the values of the quadrupolar coupling constant e^2qQ_n/h and the asymmetric parameter η of a triangle borate with a nonbridging oxygen, which provided the best fit for CBS. However, the calculated pattern was far from the observed pattern with respect to the modulation amplitude. Next, we assumed that B^{3+} ion takes the tetrahedral coordination with four bridging oxygens directly bonding to P^{5+} ions as is seen in crystalline BPO_4. Then, an excellent agreement was obtained between the observed and calculated patterns. The optimized values of e^2qQ_n/h and η were 1.66 MHz (^{10}B) or 0.80 MHz (^{11}B) and zero, respectively. These values are within the range of reported values for the tetrahedrally coordinated boron.[12] The r and N values for P^{5+} ions were similar to those in CPS. On the other hand, the best fitted result on B^{3+} was obtained when four B^{3+} tetrahedral ions were positioned at 0.45 nm (r_{B1}=0.45 nm, N_{B1}=4), and 2 B^{3+} tetrahedral ions were at 0.55 nm (r_{B2}=0.55 nm, N_{B2}=2). The configuration deduced is illustrated in Fig. 5 (right). When the coordination of boron was changed from a tetrahedral to a triangle, no satisfactory agreement was obtained as shown in Fig. 5. The separation of P^{5+}–B^{3+} is 0.27 nm, which is comparable to that of P^{5+}–B^{3+} in crystalline BPO_4. These results denote that the "solvation shell" structure[7] formed by the P^{5+} doping is also seen in the silica glass simultaneously doped with P^{5+} and B^{3+} ions.

It is worth noting that such a unique coordination of Ce^{3+}

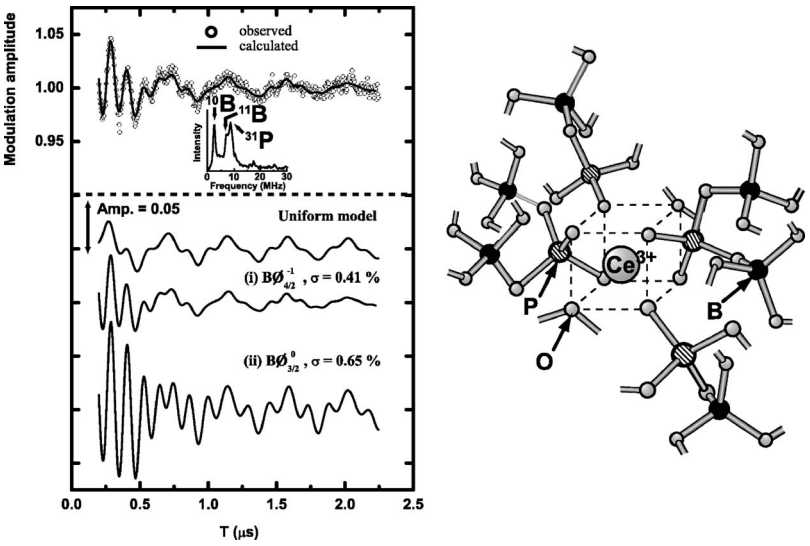

FIG. 5. Observed and calculated ESEEM patterns for CPBS sample (left) and the model. The measurement conditions; $\tau=172$ ns and $H_0=500$ mT, and 4 K. (Top) observed and best-fitted patterns. The best-fitted pattern was obtained for the case that two P^{5+} ions are positioned at 0.28 nm from a Ce^{3+}, two P^{5+} ions at 0.38 nm, four tetrahedral B^{3+} ions at 0.45 nm, and two tetrahedral B^{3+} ions at 0.55 nm. Here, each B nucleus has the quadrupolar coupling constant e^2qQ_n/h of 1.66 MHz for ^{10}B or 0.80 MHz for ^{11}B, and has the asymmetry parameter η of zero. The standard deviation of the fitting σ is 0.41%. (Bottom) patterns calculated for the uniform (P+B) distribution and the best-fitted model. (ii) is the pattern for the model modified by only changing the boron coordination number (tetrahedral→triangle).

as seen in $CePO_4$ is realized in SiO_2 glass only by the doping of 1 mol % P_2O_5. Also to be noted is that edge-sharing coordination, which is unusual in glass, occurs at the fraction comparable to a corner-sharing coordination. The total number of P^{5+} ions in the solvation shell estimated was four from the ESEEM analysis, but the average number calculated from the uniform distribution was 0.4. Therefore, the selectivity of P^{5+} ions to a Ce^{3+} is evaluated to be ~10 over Si^{4+} ions. This result provides a direct evidence for the formation of a solvation shell around a Ce^{3+} by phosphorus doping. On the other hand, the present result revealed that Ce^{3+}-B^{3+} spacing was 0.30 nm and the number of B^{3+} ions was 0.8. The average number expected from uniform distribution was 0.8. Thus, the selectivity of B^{3+} ions was ~1 over Si^{4+} ions, i.e., the "solvation shell" structure is not created by boron doping. It is of interest to note that although the number of boron evaluated in the coordination sphere of Ce^{3+} is close to that calculated from uniform distribution of boron, the ESEEM pattern calculated for the uniform distribution model is distinctly different from the observed pattern (Fig. 4). This means that the number of boron in the second neighboring coordination is rather definite, i.e., the major faction of the coordination sphere of a Ce^{3+} involves a $BOØ^{-1}_{2/2}$ unit. Further, simulation of the observed ESEEM pattern revealed that the number and position of P^{5+} ions in CPBS is the same as that in CPS, and a tetrahedral boron with four bridging oxygens is directly linked to such a PO_4 unit. This linkage close to the BPO_4-type structure implies that the formation energy of such a silica-analog structural unit is large. This idea is consistent with a recent finding reported for sodium borophosphate glasses.[16] Although B^{3+} ions are preferentially involved in the coordination sphere up to the fourth neighboring position, no B-O bond directly coordinates to a Ce^{3+} as a result of competition with P-O bonds.

Last, the relationship between the coordination structure and optical properties of Ce^{3+} is discussed. The energy level of the Ce^{3+} 5*d* multiplets is primarily determined by the electronic state of the oxygen 2*p* orbitals. There are three types of oxygen ligands with different charge states in the present samples; a bridging oxygen (formal charge=0), a nonbridging oxygen (−1), and a nonbridging oxygen of the $PO_2Ø^{-1}_{2/2}$ group (−1/2).[17] The energy splitting of the Ce 5*d* multiplets should increase with the negative charge on the ligand oxygens. Thus, energy separation between the emitting excited state (the lowest energy level among the crystal field split 5*d* multiplet) and the ground state $(4f)^1$ increases with the reduction of the negative charge density on the ligand. This idea agrees with the experimental results, i.e., Ce^{3+} coordinated by the P-O bonds gives rise to UV PL, while Ce^{3+} with B-O and Si-O bonds yields blue PL.

[1] L. Skuja, J. Non-Cryst. Solids **239**, 16 (2000).
[2] R. Brückner, in *Silicon Dioxide in Encyclopedia of Applied Physics*, edited by G. L. Tigg (VCH Verlag, Berlin, 1997), Vol. 18, pp. 101–131.
[3] H. Hosono *et al.*, Phys. Rev. Lett. **87**, 175501 (2001).
[4] Y. Ikuta *et al.*, Appl. Phys. Lett. **80**, 3916 (2002).
[5] K. Arai *et al.*, J. Appl. Phys. **59**, 3430 (1986).
[6] Y. Ishii *et al.*, J. Am. Ceram. Soc. **70**, 72 (1987).
[7] K. Arai *et al.*, J. Non-Cryst. Solids **95&96**, 609 (1987).
[8] S. Sen *et al.*, J. Appl. Phys. **89**, 2304 (2001).
[9] A. Schweiger and G. Jeschke, *Principles of Pulse Electron Paramagnetic Resonance* (Oxford University Press, Oxford, 2001); S. Sen *et al.*, J. Non-Cryst. Solids **333**, 22 (2004).
[10] S. Matsuishi *et al.*, J. Phys. Chem. B **108**, 18557 (2004).
[11] Y. -X. Ni *et al.*, Am. Mineral. **80**, 21 (1995).
[12] P. J. Bray, Inorg. Chim. Acta **289**, 158 (1999).
[13] Y. H. Yun and P. J. Bray, J. Non-Cryst. Solids **27**, 363 (1978).
[14] D. L. Griscom, J. Chem. Phys. **55**, 1113 (1971).
[15] Y. Deligiannakis *et al.*, Phys. Rev. B **58**, 11420 (1998).
[16] M. Zeyer-Düsterer *et al.*, Solid State Nucl. Magn. Reson. **27**, 50 (2005).
[17] In a middle phosphate group, an electron is delocalized over two nonbridging oxygens via $p\pi$-$d\pi$ bonding. As a result, the formal charge on the nonbridging oxygen is −1/2.